------ Raf. Jou. Sci., Vol. 22, No.2 pp 50- 57, 2011------

Geometrical Effects on the XRF Spectrometer Data Validity Using Hypothetical 20 keV Photon Source

Sabeeh K. Shamoon
Department of Physics
College of Science
Mosul University

(Received 30 / 9 / 2010 ; Accepted 27 / 12 / 2010)

ABSTRACT

The factors associated with source – sample – detector geometry and radiation absorption by 2 cm in diameter circular carbon samples on the x-ray fluorescence spectrometer data validity is studied. Radiation coming out from various parts of the sample may not share in equal manner to the detector signal if the geometry is not calculated correctly. This case may also arise if a sample is not homogeneous, so if correct geometry is designed the decision on sample homogeneity can be made. Carbon samples of 30 mg/cm^2 are supposed and suitable distance from 20 keV hypothetical photon source and detector were found in a search to solve the geometry problem.

Keywords: *XRF fluorescence, Carbon sample, Geometrical effect.*

التأثيرات الهندسية على صحة معطيات مطياف الأشعة السينية التفلورية باستخدام مصدر فوتوني مفترض 20 keV

الملخص

تمت دراسة العوامل الهندسية المرتبطة بأبعاد المصدر ـ النموذج ـ الكاشف وامتصاص الأشعة بواسطة نماذج كاربونية دائرية بقطر 2 cm وتأثير هذه العوامل على صحة معطيات مطياف الأشعة السينية التفلورية. الأشعة المنبعثة من الأجزاء المختلفة للنموذج قد لا تساهم بشكل متساوٍ في إشارة الكاشف أذا لم يتم حساب العوامل الهندسية بشكل صحيح ، وممكن أن تنشأ هذه الحالة إذا كان النموذج غير متجانس. وهكذا إذا تم حساب العوامل الهندسية بشكل صحيح فمن الممكن تقدير فيما إذا كان النموذج متجانساً آم لا. عدت نماذج كاربونية (30 mg/cm^2)، وتم إيجاد المسافات لهذه النماذج من المصدر الفوتوني المفترض (20 keV) ومن الكاشف وذلك لآجل حل مسألة العوامل الهندسية .

الكلمات الدالة: الأشعة السينية, عينة الكاربون، التأثير الهندسي.

INTRODUCTION

X-ray fluorescence (XRF) analytical technique is well known method for multielement analysis of a wide variety of samples(Stanzenieks *et al*., 1978) ; (Sood *et al*., 1983). The problem source-sample-detector geometry resulting in different quantities of radiation emitted from the sample has been solve recently by (Mahrok and Shamoon, 2008) . But the energy they used was 661.6 keV.

However, another authors (Midley *et al.,* 2005) ; (Han *et al*., 2009) ; (Van Espen *et al*., 1979). Use M_o characteristics K-X-ray , 17.4 keV or Ag characteristics K-X-ray, 22 keV in their spectrometers. This is because photo electric absorption and consequently the emission of fluorescent photons from the sample is dominate at low photon energy. Therefore, the geometry associated problems of the (XRF) spectrometer by using 20 keV hypothetical photon source was attempted.

PROCEDURE

Circular sample 2 cm in diameter with carbon surface density of 30 mg/cm^2 were considered . Due to sample finite size , Photons will travel along different path both from source to sample and from sample to detector see fig. (1)

In order to examine the effects of these factors on the homogeneity of radiation received by the detector, 3 points on sample surface were consider and irradiated by hypothetical photon source (20 keV) and the intensities were calculated of radiation arriving at these points using the inverse square law. Then the intensities of scattered radiation (elastic and inelastic) received by the detector from these 3 points were calculated by equations given in (Van Espen *et al* ., 1979)

$$N_E = I_o G \varepsilon_E t_E S_E(\rho x) \quad \text{..... (1)}$$

$$N_I = I_o G \varepsilon_I t_I S_I(\rho x) \quad \text{.....(2)}$$

Where N_E and N_I are the number of counts in elastic and inelastic scatter peaks respectively; I_o is the number of the photons incident on the sample during the measurement time. Auto CAD program was employed to calculate the radiation path lengths from the source to 3 points on the sample (d_1,d_2,d_3) and from these point to detector (D_1, D_2 ,D_3) . Table (1) shows calculated data for a 2 cm diameter sample.

Table 1: Distance from sample (2 cm in diameter) to source and detector.

Source – sample distance (cm)			**Sample – detector distance (cm)**		
d_1	**d_2**	**d_3**	**D_1**	**D_2**	**D_3**
1.4736	2	2.7979	2.7979	2	1.4736
3.3679	4	4.7599	4.7599	4	3.3679
5.3399	6	6.7443	6.7443	6	5.3399
7.3271	8	8.7358	8.7358	8	7.3271
9.3118	10	10.7304	10.7304	10	9.3118
11.3150	12	12.7268	12.7268	12	11.3150

Then the radiation intensity arriving at 3 points on the sample was calculated using the inverse square law and tabulated in Table (2) .

Table 2: Radiation intensity arriving at 3 points on the sample (2 cm in diameter).

Source – sample distance (cm)			**Radiation intensity at the sample in terms of (I_o)**		
d_1	**d_2**	**d_3**	**I_1**	**I_2**	**I_3**
1.4736	2	2.7979	0.4605	0.25	0.1277
3.3679	4	4.7599	0.08817	0.0625	0.044137
5.3399	6	6.7443	0.03507	0.027777	0.021985
7.3271	8	8.7358	0.018627	0.015625	0.013104
9.3118	10	10.7304	0.011513	0.01	0.008685
11.3150	12	12.7268	0.007811	0.006944	0.006174

The geometrical factor G for the point source is given in [Mahesh and Mustafa,1978]

$$G = \frac{r^2}{4D^2} \qquad \text{…… (3)}$$

Where (r) is the radius of Si(Li) circular face. (D) is the distance from the sample to the detector. The factor (G) was calculated for r =2.82 cm and shown in Table (3).

Table 3: The (G) for distance between the 3 points on sample and detector.

Sample-detector distance (cm)			**Geometry factor**		
d_1	**d_2**	**d_3**	**G_1**	**G_2**	**G_3**
1.4736	2	2.7979	0.253965	0.497025	0.915544
3.3679	4	4.7599	0.087749	0.124256	0.175275
5.3399	6	6.7443	0.043708	0.055225	0.069722
7.3271	8	8.7358	0.026052	0.031064	0.037032
9.3118	10	10.7304	0.017267	0.019881	0.022889
11.3150	12	12.7268	0.012274	0.013806	0.015528

Thin silicon detector of (3 mm) thick active layer of Si 25 mm^2 in area is assumed. The detector entrance window is 0.025 mm of Be (1 ml). The detector efficiency is calculated using equation (4) (Jenkins,1988) and plotted in Fig.(2), which is very similar to Canberra efficiency curve

$$\varepsilon(E) = \exp(-\mu_{Be}(E)\,\rho_{Be}\,X_{Be})\,(1-\exp(-\mu_{Si}(E)\,\rho_{Si}\,X_{Si})) \qquad \text{…….(4)}$$

Where μ_{Be} is the mass attenuation coefficient of Be = 0.2232 cm^2/gm, μ_{Si} is the mass attenuation coefficient of Si = 4.3737 cm^2/gm at 20 keV, X_{Si} is the thickness of active layer of Si = 0.5 cm, X_{Be} is the thickness layer of Be = .0025 cm, $\varepsilon(E)$ is the detector

efficiency, ρ_{Be} is the density of Be = 1.85 g/cm^3 , ρ_{Si} is the density of Si = 2.42 g/cm^3, The efficiencies of elastically ε_E and in elastically ε_I scattered radiation were obtained from this curve taken from (Canberra [8]ed) interpolation ε_E = 95% for 20 keV and ε_I = 97% for 19.247 keV.

t_E and t_I are the absorption correction factors for the elastic and inelastic scatter radiation respectively(Van Espen *et al.*, 1979).

$$t_E = \frac{1-\exp\left(-2\mu_E \, csc\emptyset \, (\rho x)\right)}{2\mu_E csc\emptyset(\rho x)} \qquad \text{.....(5)}$$

$$t_I = \frac{1-\exp(-\mu_E+\mu_I)csc\emptyset(\rho x))}{(\mu_E+\mu_I)csc\emptyset(\rho x)} \qquad \text{.....(6)}$$

Where μ_E = total mass absorption coefficient in cm^2/gm for 20 keV; μ_I= total mass absorption coefficient in cm^2/gm for 19.247 keV . $\emptyset$ = 45^o which is the angle that the sample surface makes with exciting radiation and with radiation scattered to the detector. Values of μ_E and μ_I for carbon at 20 keV were interpolated from the tabulation of (Storm and Israel, 1970). The values found are μ_E = 0.4322 cm^2/gm at 20 keV and μ_I = 0.44 cm^2/gm for 19.247 keV which is the energy of the in elastically scattered photon. Putting the values μ_E , μ_I, $\emptyset$ and (ρx)= 30 mg/cm^2 in equation (5) and (6).

The correction factors t_E and t_I were found to be 0.9819 and 0.9818 respectively which quite close to one but can not be neglected .

The elastic and inelastic scatter cross-sections σ_E and σ_I are plotted against the atomic number Z for 20 KeV photons by interpolation of the theoretical data given in (Hubbell *et al.*, 1975) and shown in fig.(3) and fig.(4) The scatter cross-sections σ_E and σ_I are expressed as:

$$ln\sigma_E = 1.39\, lnZ + B \qquad \text{.....(7)}$$

$$ln\sigma_I = -0.29\, lnZ + D \qquad \text{.....(8)}$$

B and D are y-intercepts for σ_E and σ_I respectively. The scatter factor S_E and S_I depends on x-ray energy and atomic number of the sample elements. These factor were found theoretically from equation (7) and (8) as :

$$S_E = Z^{1.39} \quad \text{and} \quad S_I = Z^{-0.29}$$

If the counts (of one energy value) received by the detector from different point on sample are similar, then the geometrical arrangement of XRF analyzer are correct.

The application of this condition to more than one energy value received by the detector, gives better confidence about the geometry.

When d ≠ D, values of N_E arriving at the detector from 3 points on the sample were found to be different, and so were values of N_I , therefore all cases for which d ≠ D are ignored. When d = D = 2 to 12 cm, values of N_E and N_I were calculated in step of 1 cm and some of these are shown in Table (4). When d = D < 6 cm N_E values corresponding to 3pionts on sample are dissimilar, and so are values of N_I. further to that, values of $N_{E1} \approx N_{E3} < N_{E2}$ and $N_{I1} \approx N_{I3} < N_{I2}$. this is attributed to the distances (which are not equal) covered by radiation inside the sample when traveling to and from points1, 2, and 3 in all the cases of d = D < 6 cm .

However, these distance seem to home similar effects on both N_E and N_I values and d = D ≥ 6 cm .Table (4). N_E and N_I values calculated using hypothetical 20 keV photon source and 2 cm diameter carbon sample of 30 mg/cm^2 where d = D.

Table 4: N_E and N_I Values calculated using hypothical 20 keV photon source and 2 cm diameter carbon sample of 30 mg/cm^2 when d=D.

Sample-detector distance (cm)			N_{E1} x 10^{-6}	N_{E2} x 10^{-6}	N_{E3} x 10^{-6}	N_{I1} x 10^{-6}	N_{I2} x 10^{-6}	N_{I3} x 10^{-6}
d_1	**d_2**	**d_3**						
1.4736	2	2.7979	40284	42800	40271	1989	2114	1989
3.3679	4	4.7599	2665	2675	2665	131	132	131
5.3399	6	6.7443	528	528	528	26	26	26
7.3271	8	8.7358	167	167	167	8	8	8
9.3118	10	10.7304	68	68	68	3	3	3
11.3150	12	12.7268	33	33	33	2	2	2

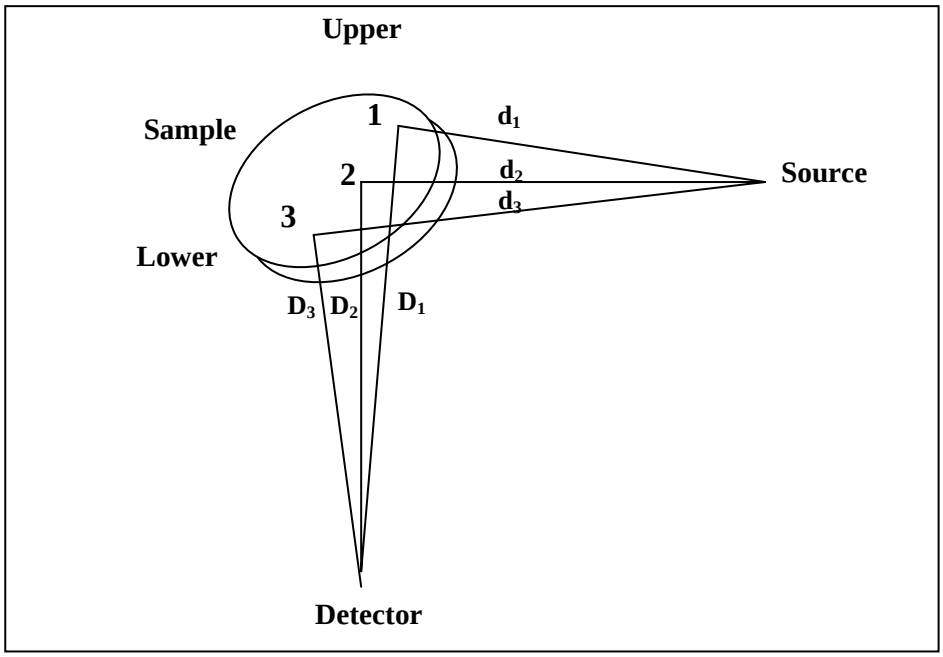

Fig. 1: Illustration of different radiation path from source- sample- detector geometry arbitrary scale.

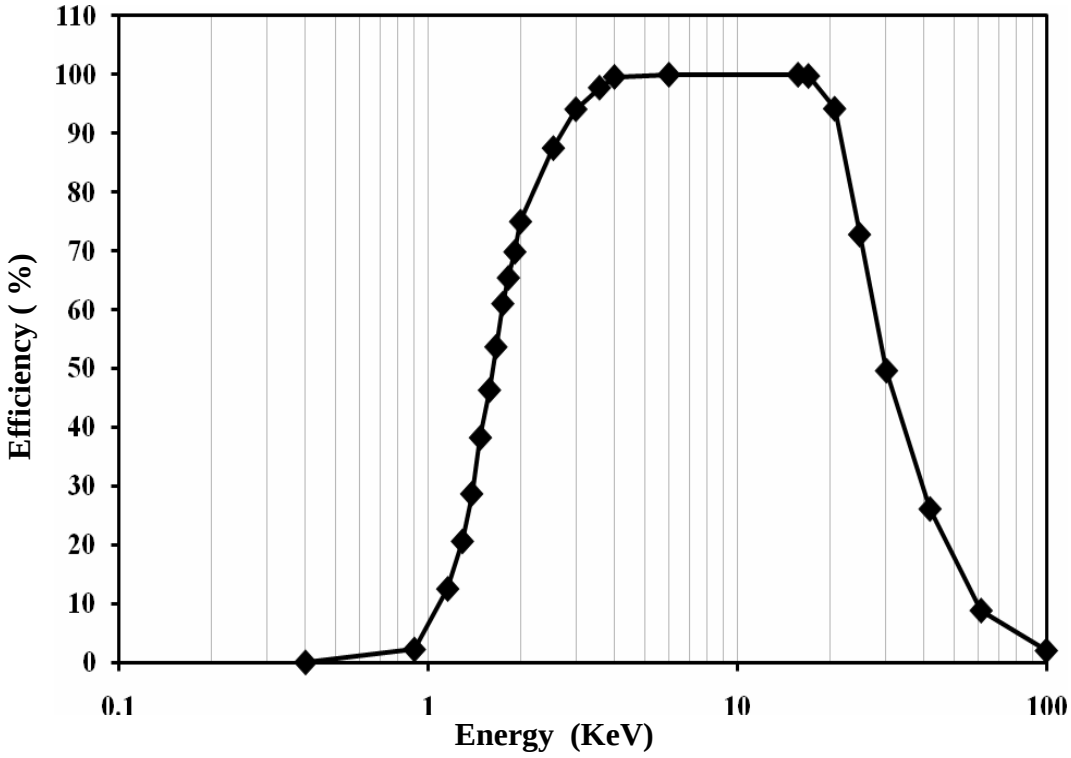

Fig. 2: Efficiency as a function of the incident photon energy (keV)

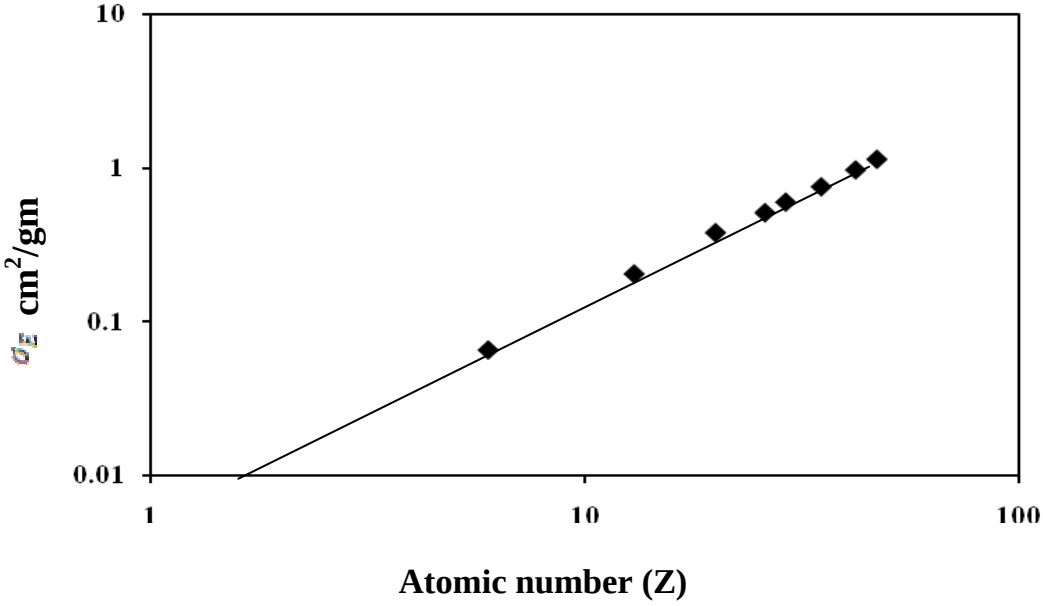

Fig. 3 : σ_E Vs atomic number

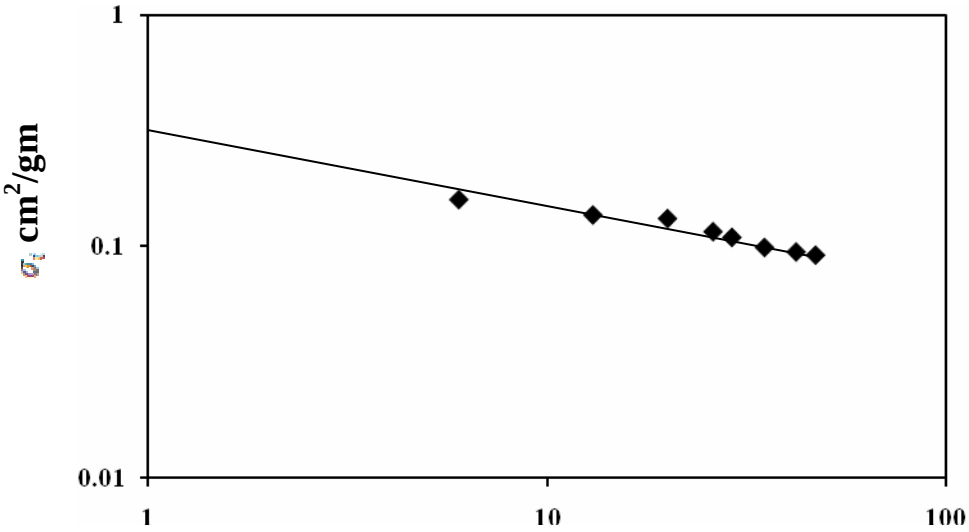

Fig. 4 σ_i Vs atomic number

DISCUSSION

Reliable result are usually required from any XRF spectrometer. Radiation (N_E or N_I) emitted from and scattered by various parts of the sample may not contribute in equal manner to the detectors signal if either the geometry of the spectrometer is misdesigned or the sample is not homogeneous, or both.

Sample in homogeneity arises from variation in thickness, and / or density along the sample. However, geometric configuration could have negative effects on the sample analysis result if not correctly designed .

Hence, decision on homogeneity can only be made if the effect of the spectrometer geometry is eliminated such that similar values of N_E and of N_I arrive at the detector. In this work, the distances d = D ≥ 6 cm were found to be adequate for the 90^o mode of excitations; other values may be obtained for different energies, spectrometric configurations, and sample sizes.

In this current work, by using a new detector source and according to a suitable geometrical configuration, results show close approximation to current condition d= D ≥ 6 with previous results (Mahrok and Shamoon, 2008) which we obtained then d= D ≥ 8. We conclude by comparing the two results that d= D ≥ 8 is an optimum condition for all energies and detector types.

REFERENCE

Canbera cataloge. Nuclear product group Edition Eight. One state strict Meriden CT 06450.

Han, I. ; Demir, L. (2009). "Determination of Mass Attenuation Coefficients, Effective Atomic and Electron Number for Cr, Fe and Ni Alloys at Different Energies". Nuclear Instrument and Methods in physics Research .B 276, pp. 3-8.

Hubbell, J. H.; Veigele, W_m. J.; Briggs, E. A.; Brown, R. J.; Gromer D. T.; Howerton, R. J. (1975). Atomic from factors, Incoherent Scattering Functions and photon scattering cross section, *J. Phys. Chem. Ref. Data* , **4**, (3), 471- 538 .

Jenkins, R. (1988). "X-Ray Fluorescence Spectrometry". John Wiley and Sons. pp.1-18.

Mahesh, K.; Mustafa, S.M. (1976). "Nuclear Radiation Detector and Experiment", Mosul University press. pp. 115-121.

Mahrok, M.; Shamoon, S. (2008). The effect of geometrical factors on the XRF spectrometer data validity . *J. Applied Spectroscopy* . **75** (2), 280-283.

Midley, S. M. (2005). Measurement of the X-Ray linear attenuation coefficient for low atomic number materials at energies 32-66 and 140 keV, *Radiation Physics and Chemistry*. **72,** 525-535.

Sood, B. S. ; Allawadhi, K. L.; Gandi, R.; Batra, O.P. ; Singh, N. (1983). Sample analysis using gamma-ray induced fluorescent X–ray- emission, *X-Ray Spectrometry* . **12**, (1), 19-22.

Stanzenieks, P. ; Rinby, A. ; Selin, E. (1978). Development of a law power Mono-Energetic X- ray Tube for Trace Element Analysis , *Nuclear Instruments and Methods*, **153**, 269-276.

Storm, E.; Israel. H.I. (1970). Photon Cross- Section from 1 keV For Elements, Z=1 to Z=100 , *Nuclear Data Table's* A7, 565-681.

Van Espen, P.; Van'Dack, L. ; Adams, F.; Van Grieken R. (1979). Effective Sample Weight From Scatter Peaks in Energy Dispersive X-Ray Fluorescence. *Anal. Chem*., **51** (7), 961-967.